Functional 3D Human Liver Bud Assembled from MSC-Derived Multiple Liver Cell Lineages

Jing Li[1], Feiyue Xing[1], Feng Chen[2], Liumin He[3], Kwok-Fai So[4], Yingxia Liu[2], and Jia Xiao[2,4]

Abstract

The severe shortage of donor liver organs requires the development of alternative methods to provide transplantable liver tissues such as stem cell-derived organoids. Despite several studies describing the generation of vascularized and functional liver tissues, none have succeeded in assembling human liver buds containing hepatic stellate cells (HSCs) and liver sinusoidal endothelial cells (LSECs). Here, we report a reproducible, easy-to-follow, and comprehensive self-assembly protocol to generate three-dimensional (3D) human liver buds from naïve mesenchymal stem cells (MSCs), MSC-derived hepatocytes, and HSC- and LSEC-like cells. By optimizing the ratio between these different cell lineages, the cell mixture self-assembled into 3D human liver buds within 72 h *in vitro*, and exhibited similar characteristics with early-stage murine liver buds. In a murine model of acute liver failure, the mesenteric transplantation of self-assembled human liver buds effectively rescued animal death, and triggered hepatic ameliorative effects that were better than the ones observed after splenic transplantation of human hepatocytes or naïve MSCs. In addition, transplanted human liver buds underwent maturation during injury alleviation, after which they exhibited a gene expression profile signature similar to the one of adult human livers. Collectively, our protocol provides a promising new approach for the *in vitro* construction of functional 3D human liver buds from multiple human MSC-derived hepatic cell lineages; this new technique would be useful for clinical transplantation and regenerative medicine research.

Keywords

human liver bud, organoid, mesenchymal stem cell, acute liver failure

Introduction

Chronic liver disease is characterized by the progressive destruction and declining regeneration of hepatic tissues, which give rise to the development of fibrosis and possibly cirrhosis if these damages are not mitigated. It is one of the major causes of mortality worldwide. In 2013, chronic liver disease and cirrhosis caused 36,427 deaths across all age groups in the United States[1]. Clinically, liver transplantation is the only definitive treatment for end-stage liver diseases, including acute liver failure, cirrhosis, and liver cancers[2]. However, the critical shortage of donor liver organs and the severe graft rejections highlight the urgent need for the generation of liver organs from autologous stem cells, which have the capacity for self-renewal, immune-regulation, homing instinct, and regeneration[3]. Moreover, stem cell transplantation can overcome the major limitations of direct hepatocyte transplantation, such as organ availability, limited cell proliferation, loss of function, and the risk for immune rejection[4].

One of the major defects associated with the use of resuspended stem cells or stem cell-derived hepatocyte injection is the risk for phenotypic and functional deficiencies (e.g., loss of cellular cuboidal morphology and of

---

[1] Department of Immunobiology, Institute of Tissue Transplantation and Immunology, Jinan University, Guangzhou, China
[2] State Key Discipline of Infectious Diseases, Shenzhen Third People's Hospital, Shenzhen, China
[3] Key Laboratory of Biomaterials of Guangdong Higher Education Institutes, Department of Biomedical Engineering, Jinan University, Guangzhou, China
[4] School of Biomedical Sciences, University of Hong Kong, Hong Kong SAR

Corresponding Authors:
Jia Xiao and Yingxia Liu, State Key Discipline of Infectious Diseases, Shenzhen Third People's Hospital, No. 29, Bulan Road, Longgang District, Shenzhen, 518112, China.
Emails: edwinsiu@connect.hku.hk; yingxialiu@hotmail.com

liver-specific functions, such as decreased secretion of albumin and impaired phase I and II enzymatic detoxification abilities, were frequently observed)[5]. Despite many studies reporting the amelioration of various liver diseases by using naïve stem cell or stem cell-derived hepatocyte transplantation, including acute liver failure[6], chronic hepatitis B (CHB)[7], chronic hepatitis C (CHC)[8], alcoholic liver disease (ALD)[9], drug-induced liver injury (DILI)[10], primary biliary cirrhosis (PBC)[11], severe cirrhosis[12], and hepatocellular carcinoma (HCC)[13], few studies have described the generation of functional three-dimensional (3D) liver buds assembled entirely from stem cells or stem cell-derived liver cells, which could be directly transplanted to alleviate liver injury and promote liver regeneration[14]. More importantly, no studies have reported the generation of 3D liver buds with functional hepatic stellate cells (HSCs) and liver sinusoidal endothelial cells (LSECs). To facilitate future clinical applications of direct transplantation, in the current study we aimed to establish a comprehensive and reproducible method to generate functional 3D human liver buds based on self-condensation mechanisms of different liver cell types derived from human mesenchymal stem cells (hMSCs). We also validated the transplantation capacity of self-assembled human liver buds in a model of immunodeficient mice with liver injuries. The maturation capacity of liver bud transplants was also investigated.

Materials and Methods

Hepatocyte Differentiation

Hepatocyte differentiation from human umbilical cord blood stem cells (hUCBSCs) was conducted using a StemXVivo Hepatocyte Differentiation Kit (R&D Systems, Minneapolis, MN, USA). Briefly, before the induction of differentiation, wells of cell culture plates were precoated with Cultrex® Stem Cell Qualified Reduced Growth Factor (RGF) Basement Membrane Extract (BME) (Trevigen, Gaithersburg, MD, USA) for 2 h and then seeded with hUCBSCs at a density of $1.1–1.25 \times 10^5$ cells/cm^2 and cultured in MEF-conditioned media containing basic fibroblast growth factor (bFGF). hUCBSCs were sequentially treated with differentiation medium numbers 1, 2, 3, and 4 for 5, 4, 4, and 5 days, respectively.

Differentiated Hepatocyte Function Tests

Differentiated hepatocytes were treated with 20 μM beta-naphthoflavone (BNP) for 24 h to induce cytochrome P450 1A1 (CYP1A1) expression. Then, cells were incubated for 30 min in methoxyresorufin, a CYP1A1 substrate that produces the fluorescent metabolite resorufin. The absorbance of resorufin was detected at 570 nm on a plate reader. To measure the induction of cytochrome P450 3A4 (CYP3A4), differentiated hepatocytes were treated with either 50 μM dexamethasone or 25 μM rifampicin for 48 h. The cellular activity of CYP3A4 was measured by using a P450-Glo CYP3A4 cell-based assay kit (Promega, Madison, WI, USA) following the manufacturer's instructions.

To further prove the function of differentiated hepatocytes, cells were treated with acetaminophen (APAP, 1 mM or 10 mM, in ethanol) for 24 h. Normal culture medium with ethanol was set as the control group. Treated cells were assessed by the Resazurin metabolism assay (R&D Systems, cat.: AR002), which generated a cumulative increase in fluorescence over time.

HSCs and LSECs Co-Differentiation

Passage 3 hUCBSCs were seeded at an approximate density of 1×10^5 cells/cm^2 and cultured in DMEM/F-12 medium supplemented with 1 μM dexamethasone, $0.25\times$ ITS (insulin, transferrin, selenium), and 0.5% FBS (fetal bovine serum) (all from Sigma-Aldrich, Shanghai, China). The co-differentiation of HSC and LSEC consisted of a sequential four-step supplementation protocol with the following factors: (1) from day 1 to day 6: 40 ng/ml Wnt3a and 75 ng/ml Activin A; (2) from day 7 to day 10: 5 ng/ml bFGF and 25 ng/ml bone morphogenetic protein 4 (BMP4); (3) from day 11 to day 14: 25 ng/ml acidic FGF, 5 ng/ml FGF4, and 20 ng/ml FGF8; and (4) from day 15 to day 28: 10 ng/ml hepatocyte growth factor (HGF) and 50 ng/ml Follistatin. All supplementation factors were bought from R&D Systems. Matrigel was not used to precoat the bottom of the culture plates or wells (i.e., non-coated plates). The cell morphology was recorded every day for each group. All cell culture methods, including the incubation duration, the selection and concentration of each supplement, and the coating conditions were optimized based on our pilot studies. Differentiated HSC- and LSEC-like cells were subsequently subjected to cell sorting, analysis, and self-assembly.

Flow Cytometry

To sort and analyze HSC-like cells after the induction of hUCBSCs differentiation, cells were treated for 24 h with 5 μM vitamin A, which is stored in HSC-like cells as retinyl esters contained in cytosolic lipid droplets[15]. Fluorescent cells [Indo-1 (Violet)-A positive] were analyzed and sorted from the hUCBSCs/HSCs/LSECs pool by fluorescence-activated cell sorting (FACS) (BD FACSVerse, BD Biosciences, San Jose, CA, USA)[16]. For LSEC-like cell selection, cells were sorted and analyzed from mixed cultures by using VE-cadherin or isotype control antibodies (R&D Systems).

Fluorescent Microscopy

After vitamin A incubation, live HSC-like cells containing stored retinyl esters emitted blue fluorescence under ultraviolet light stimulation, which was detected by inverted fluorescence microscope IX71 (Olympus Microscope, Tokyo, Japan). Similarly, VE-cadherin expressing LSEC-like cells were detected by performing immunofluorescence

assay. Cells were fixed with 4% formaldehyde (v/v) at room temperature for 15 min and then permeabilized with 1% Triton X-100 in Tris buffer (Gibco, Waltham, MA, USA) for another 15 min. To block nonspecific antibody binding sites, cells were treated with phosphate-buffered saline (PBS) solution containing 5% bovine serum albumin (BSA) for 1 h at 37°C. Subsequently, cells were incubated in the same solution containing the VE-cadherin primary antibody (1:100 dilution) for 2 h at room temperature. After three washes with PBS, cells were incubated for 1 h with the secondary antibody goat anti-mouse IgG conjugated with FITC (1:1000, Abcam Asia, Hong Kong, China) at room temperature. To visualize nuclei, cells were counterstained with Hoechst 33342 (Beyotime, Jiangsu, China) for 15 min at room temperature. Slides were mounted with fluorescent mounting medium (KPL, Gaithersburg, MD, USA) before microscope examination.

Self-Assembly of Human Liver Buds from Multiple Cell Lineages

To achieve the self-assembly of human liver buds from multiple cell lineages *in vitro*, 1×10^6 differentiated hepatocytes, 0.3×10^6 differentiated HSC-like cells, 0.3×10^6 differentiated LSEC-like cells, and 0.1×10^6 undifferentiated hUCBSCs were resuspended together in DMEM/F-12 medium containing 2.5% FBS, 50 nM dexamethasone, 10 ng/ml Oncostatin M, and 5 ng/ml HGF and plated on presolidified $1 \times$ Matrigel diluted in DMEM/F-12 medium in a 24-well plate. This optimized cell lineage mixture ratio was determined based on our pilot studies (data not shown). After approximately 6 days, assembled liver buds were collected for subsequent validations and transplantations. Self-assembled liver buds, together with liver buds isolated from embryonic day 10 (E10) C57/BL6 mouse embryos (purchased from Guangdong Animal Center, Guangzhou, China), were all subjected to frozen sectioning and immunofluorescence assays using early-stage liver development markers, including CK8/18 (Abcam), AFP (Abcam), CD31 (Abcam), Desmin (Cell Signaling, Danvers, MA, USA), PCNA (Abcam), Flk1 (Cell Signaling), and BrdU (Cell Signaling).

RNA Extraction, cDNA Synthesis, and Quantitative Real-Time PCR

Total RNA was extracted from stem cells or homogenized tissues using illustra™ RNAspin mini kit (GE Healthcare, Amersham, UK) and the cDNA was generated from 2 μg of total RNA using the SuperScript™ First-Strand Synthesis System (Invitrogen, Carlsbad, CA, USA). Synthesized cDNAs were subjected to quantitative real-time PCR using the Takara SYBR premix Taq quantitative PCR system (Takara Bio Inc., Shiga, Japan) and the MyiQ2 real-time PCR machine (Bio-Rad, Hercules, CA, USA). Primer information and reaction conditions used for our quantitative real-time PCR analysis are listed in Supplementary Table 1. All quantitative real-time PCR procedures, including the design of primers, the validation of PCR conditions, and the quantification methods were performed according to the MIQE guidelines[17].

Microarray Analysis

To characterize and compare the gene expression profiles of self-assembled human liver buds with those of the corresponding murine developmental stage, we selected 83 genes that were serially upregulated during both human and mouse liver development (Supplementary Table 2) using a Whole Human Genome Agilent 4344 K v2 Oligonucleotide Microarray or a Whole Mouse Genome Agilent 4344 K v2 Oligonucleotide Microarray (Agilent Technologies, Santa Clara, CA, USA) according to the manufacturer's instructions. Briefly, total RNAs were extracted from self-assembled human liver buds, adult human liver tissues (Biochain Institute Inc., Newark, CA, USA), or CD45-negative and Ter119-negative murine liver cells from different developmental stages (E10, E13, E16, E19, postnatal day 0 [P0], and postnatal day 3 [P3]) and subjected to microarray chip hybridization. A hierarchical clustering method using Euclidean distance complete linkage on GeneSpring11.5.1 was carried out to perform cross-species comparison of gene expression profiles as previously described[18]. Similarly, to compare the gene expression profiles of self-assembled liver buds (with or without transplantation) with healthy adult human liver tissues, 38 signature genes for mature liver tissues were selected to perform a microarray analysis (Supplementary Table 3) as described above.

Transplantation

All animal experiments in the current study, including experimental procedures, sample isolations, and animal care, were approved by and in accordance with the guidelines and regulations from the ethical committee of Shenzhen Third People's Hospital (No. 2016-07). TK-NOG mice, which are mice from a highly immunodeficient strain (NOG) that express the humanized herpes simplex virus type 1 thymidine kinase (TK) transgene in their liver, with body weights ranging from 20 to 30 g, were purchased from In Vivo Science Inc. (Tokyo, Japan). Ganciclovir (Sigma-Aldrich), an antiviral medication which is not toxic to human or mouse tissues, was injected intraperitoneally to induce acute liver failure by tissue-specific ablation of transgenic liver parenchymal cells 5 and 10 days (50 mg/kg, one injection at day 5 and one injection at day 10) after the mesenteric transplantation of 10 *in vitro*-generated human liver buds. For control studies, 3×10^6 live hUCBSCs or hUCBSCs-derived hepatocytes resuspended in cold medium or cold Matrigel (BD Bioscience) respectively were transplanted into the renal subcapsular space. The mortality rate was recorded for all mice every day. Mouse liver tissues or

transplanted human liver bud tissues were collected at the end of the entire experiment for immunofluorescence and microarray analyses.

ELISA

Serum was collected from whole-blood samples of mice by centrifugation at 1000 x g for 10 min at 4°C and stored at –80°C. Serum levels of albumin and alpha 1 antitrypsin (AAT) were measured at days 0, 10, 20, and 30 post-mesenteric or splenic transplantations by using commercial ELISA kits from Abcam.

Drug Metabolism Activity Tests

To measure the drug metabolism capacity of mice transplanted with artificial liver buds, ketoprofen or debrisoquine was administered to mice as previously described[18,19]. Briefly, ketoprofen (15 mg/kg in PBS) was intravenously injected to mice at day 30 after 3D liver transplantation. Injection of vehicle PBS was set as the control group. Urine samples (0–2 h) of mice were collected with 0.5 M acetate buffer (pH 5.0) and 1 N KOH for a 3 h incubation at 80°C, which was terminated by adding an equivalent volume of 1 N HCl. Then acetonitrile containing 1% acetic acid was added to the mixture and centrifuged at 4°C, 15,000 rpm for 15 min. The supernatant was loaded to liquid chromatography-tandem mass spectrometry (LC/MS/MS, LC-20A, Shimadzu, Kyoto, Japan). The mobile phase containing 0.1% acetic acid and 0.1% acetic acid containing acetonitrile was pumped at a flow rate of 0.5 ml/min. The turbo gas was maintained at 600°C. Ionspray voltage was –4500 V and analyze m/z transitions (Q1/Q3) for ketoprofen and 1-hydroxyketoprofen were 253.1/209.3 and 269.1/209.3, respectively[18].

For the measurement of debrisoquine metabolism, a concentration of 2 mg/kg was orally administrated to mice at day 30 after transplantation. Blood samples were collected at 8 h after administration with hepatin-Na. Separated plasma was mixed with the internal standard (niflumic acid 1 μM) methanol solution and then centrifuged at 4°C, 15,000 rpm for 5 min. The following LC/MS/MS procedures were similar to that of ketoprofen. The mobile phase consisting of 10 mM ammonium acetate and acetonitrile was pumped at a flow rate of 0.8 ml/min. The turbo gas was maintained at 450°C. The ionspray voltage of the experiment was 5000 V and analyze m/z transitions (Q1/Q3) for debrisoquine, 4-hyroxydebrisoqune, and internal standard were 176.5/134.2, 192.6/132.1, and 283.2/245.4, respectively. The area under the curve from time 0 until the last measurable plasma concentration (AUC_{0-t}) was calculated using the linear trapezoidal rule. Metabolic ratios were determined by dividing AUC0-t of 4-hyroxydebrisoqune by AUC_{0-t} of debrisoquine.

Statistical Analysis

Data from each group are expressed as the mean $\pm$ SEM. Statistical comparisons between groups were done using the Kruskal–Wallis test followed by Dunn's post hoc test to detect significant differences. A value of $P < 0.05$ was considered to be statistically significant (Prism 5.0, Graphpad Software, Inc., San Diego, CA, USA).

Results

Human MSCs were Successfully Differentiated to Functional Hepatocyte-, HSCs, and LSEC-Like Cells

After 15 d of culture with a four-step differentiation protocol, hUCBSCs were successfully differentiated into mature human hepatocyte-like cells (Figure 1(a)). The differentiation efficiency was quantified by flow cytometry analysis of the cell surface hepatocyte marker, asialoglycoprotein receptor 1 (ASGPR1), which showed that differentiation of hUCBSCs resulted in approximately 74% of ASGPR1-positive hepatocyte-like cells (Figure 1(b)). After 24 h of incubation with 20 μM beta-naphthoflavone (BNP), differentiated hepatocyte-like cells were shown to express the cytochrome P450 enzyme over time (Figure 1(c)). In addition, when hepatocyte-like cells were treated with either dexamethasone (50 μM) or rifampicin (25 μM) for 48 h, evident elevation of CYP3A4 activity was observed (Figure 1(d)). We also found that a 24 h incubation with APAP made hepatocytes reduce metabolic activity, as quantified by a decreased accumulation of resorufin fluorescence over time (Figure 1(e)). These findings suggest that hUCBSCs were successfully differentiated into mature human hepatocyte-like cells.

To induce the differentiation of HSCs and LSECs, we optimized a novel 28-day, four-step co-differentiation protocol that produced HSC- and LSEC-like cells concurrently (Figure 2(a)). The morphological changes of hUCBSCs undergoing co-differentiation are presented in Figure 2(b), which shows that cells started to gain a hepatic non-parenchymal morphology at day 9 and exhibited typical HSC- and LSEC-like shapes by day 23. When cells were cultured with vitamin A and labeled with the VE-cadherin antibody, flow cytometry showed that the differentiation efficiencies of hUCBSCs into HSC- or into LSEC-like cells were approximately 21% and 19%, respectively (Figure 2(c,d)). In addition, the detection of blue fluorescent signals, which revealed the presence of retinyl esters storage in HSC-like cells (Figure 2(e)), and the significant upregulation of gene expression levels of HSC markers (*ALCAM*, *CRBP1*, *TIMP1*, and *LOX*) in sorted HSC-like cells both indicated the successful differentiation of "human HSCs" from hUCBSCs. Similarly, a small portion of the mixed cell population differentiated from hUCBSCs exhibited green fluorescence when stained with VE-cadherin antibody (Figure 2(g)). Sorted LSEC-like cells also exhibited significant high gene expression levels of typical LSEC markers (*VCAM-1*, *MRC-1*, and *CD31*) when compared with those of undifferentiated hUCBSCs (Figure 2(h)).
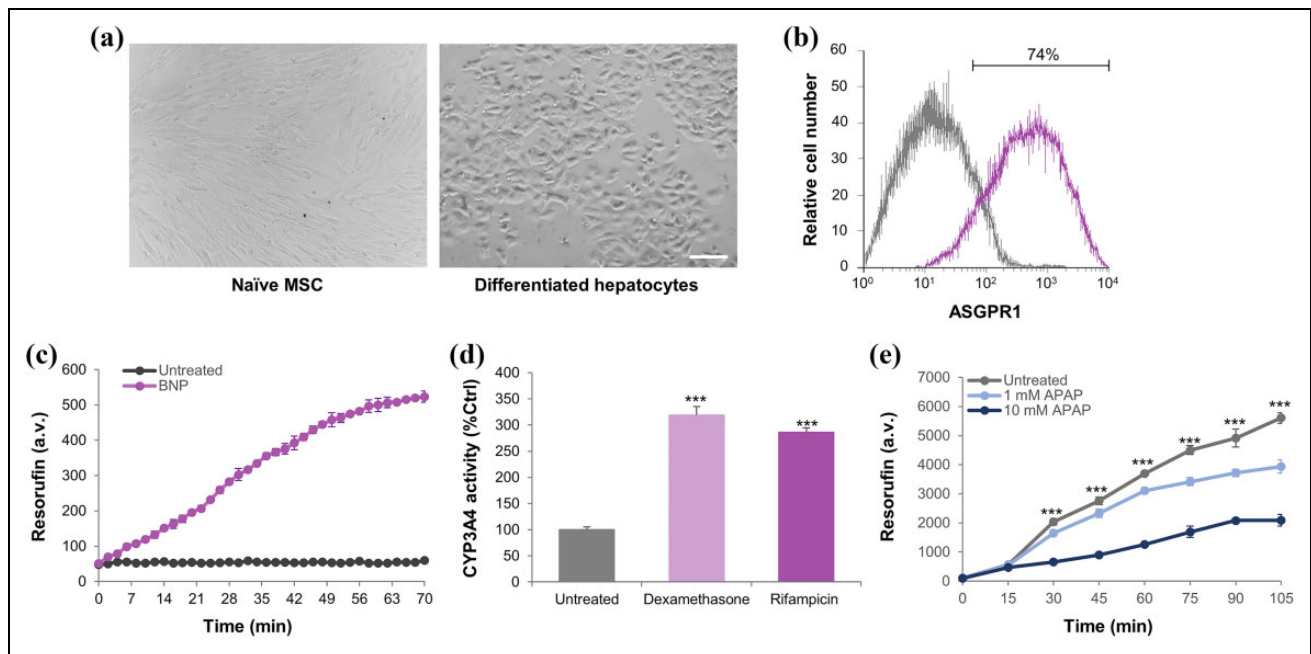
Figure 1. Functional tests of hepatocytes differentiated from human umbilical cord blood stem cells (hUCBSCs). (a) Representative cell morphology of naïve MSC and differentiated hepatocytes. (b) Differentiation efficiency was quantified by flow cytometric detection of the cell surface hepatocyte protein ASGPR1 (asialoglycoprotein receptor 1, violet histogram). Staining levels were compared to an isotype control antibody (gray histogram). (c) After a 24 h incubation with 20 μM beta-naphthoflavone (BNP), the CYP1A1 activity was determined by measuring its substrate substance 7-ethoxyresorufin in hUCBSCs-derived hepatocytes. (d) Hepatocytes were treated with either 50 μM dexamethasone or 25 μM rifampicin to induce CYP3A4 expression. (e) Hepatocytes were incubated with 1 mM or 10 mM acetaminophen (APAP) for 24 h. Accumulation of resorufin fluorescence over time was recorded. Data are presented as mean $\pm$ SEM, and significance was calculated by the Kruskal–Wallis test followed by Dunn's post hoc test (***$P < 0.001$). Scale bars, 100 μm.

Self-Assembly of Functional 3D Human Liver Buds from Mixed Cell Lineages

Since the self-assembly of functional 3D liver buds depends on the exquisite orchestration of signals among parenchymal, endothelial, and epithelial cells[20], this inspired us to generate liver buds *in vitro* by culturing hepatocyte-, HSC-, LSEC-like cells, and naïve hUCBSCs together in a 10:3:3:1 ratio for 72 h based on an optimization of the protocol used in our pilot studies (Figure 3(a)). Notably, mixed cell lineages cultured in 2D started to self-assemble 6 h post-seeding and formed visible 3D clusters (approximate diameter of 4 mm) 48 h post-seeding by intrinsic capacity for self-condensation (Figure 3(b)). After 72 h of culture, the self-assembled liver buds became mechanically stable. Quantitative real-time PCR analysis of these liver buds revealed that early hepatic markers (e.g., *ALB*, *AFP*, and *CYP3A7*) were expressed (Figure 3(c)). We also proved the indispensable roles of those four types of cell (particularly MSC and LSEC) in the self-assembly of 3D liver buds because lack of MSC or LSEC failed to form structurally functional clusters (Supplementary Figure 1). Since the formation of liver buds was initiated on the third or fourth week of gestation, which corresponds approximately to E10 for murine liver bud formation[21], we compared the protein expression of the hepatoblast marker α-fetoprotein (AFP),

the endothelial progenitor marker (CD31), and the mesenchymal progenitor marker (Desmin) between *in vitro* self-assembled human liver buds and E10 mouse liver buds by immunofluorescence. The relative expression levels and expression patterns between human and mouse liver buds were quite similar (Figure 3(d)). In addition, the analysis of cell proliferation also revealed similarities between human and mouse liver buds (Figure 3). To further characterize the gene expression profile of self-assembled human liver buds compared to those isolated from the corresponding murine developmental stage, we analyzed 83 genes that were serially upregulated during both human and mouse liver development by performing a hierarchical clustering analysis and we found that the gene expression profile of human liver buds resembled the one of E10 mouse liver buds, rather than mouse livers from advanced fetal or adult stages (Figure 3(f)). Collectively, our data suggested that by using a multi-lineage self-assemble strategy, functional 3D human liver buds were successfully generated.

Transplantation with Self-Assembled Human Liver Buds Ameliorated Murine Hepatic Injury

To facilitate future clinical application of our self-assembled human liver buds derived from stem cells, we used a
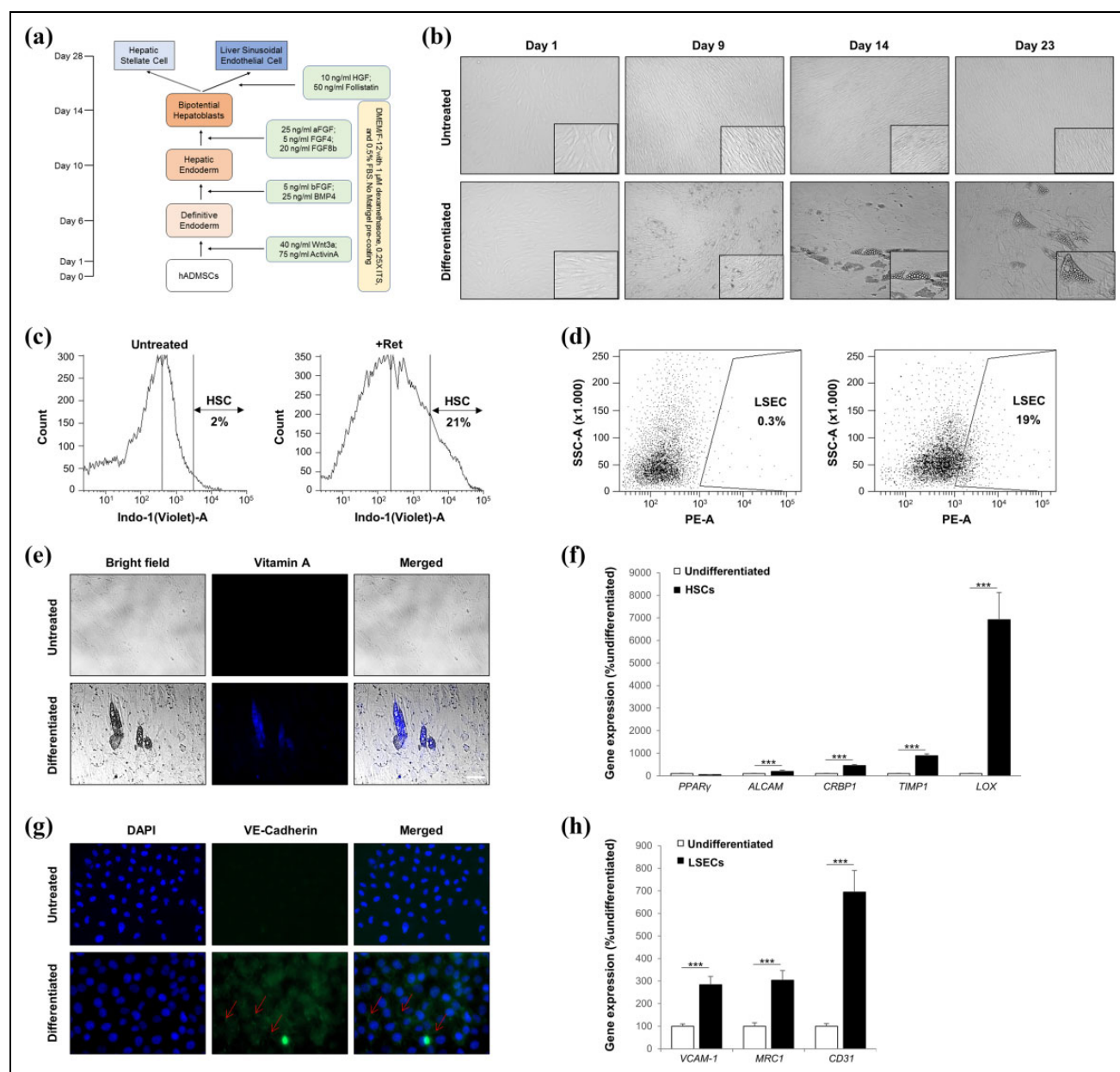
Figure 2. Co-differentiation of hepatic stellate cell (HSC)- and liver sinusoidal endothelial cell (LSEC)-like cells from human umbilical cord blood stem cells (hUCBSCs). (a) Protocols of co-differentiation. (b) Changes of cell morphology at days 1, 9, 14, and 23 during co-differentiation from hUCBSCs to HSC- or LSEC-like cells. Dotted line indicates cells have early-stage morphological changes. Solid arrow indicates HSC-like cell while hollow arrow indicates LSEC-like cell. (c) HSC-like cells were treated with vitamin A, that then is stored in stellate cells in the form of retinyl esters in lipid drops and measured by flow cytometry. Differentiation efficiency of HSC-like cells was ∼21%. (d) LSEC-like cells were isolated from mixed hUCBSCs/HSC/LSEC cultures using VE-cadherin antibody. The approximate differentiation efficiency was ∼19%. (e) Representative images of HSC-like cells held a fluorescent phenotype under UV laser excitation. (f) RNA was extracted from the Indo-1 (Violet)-A positive cells and analyzed for HSC gene expressions, including *PPARγ*, *ALCAM*, *CRBP1*, *TIMP1*, and *LOX* by quantitative real-time PCR. (g) Representative images of LSEC-like cells stained with VE-cadherin antibody. (h) RNA was extracted from the VE-cadherin-positive cells and analyzed for LSEC gene expressions, including *VCAM-1*, *MRC-1*, and *CD31* by quantitative real-time PCR. Data are presented as mean ± SEM, and significance was calculated by the Kruskal–Wallis test followed by Dunn's post hoc test (***P< 0.001). Scale bars, 100 μm.

minimal invasive mesenteric transplantation of 10 generated liver buds in TK-NOG mouse models, as previously described[18,22]. It was shown that 30 days after the concurrent gancyclovir-induced liver failure and transplantation, the group of mice with transplanted human liver buds had the highest survival rate (80%), which was superior to those of mice transplanted with human adult hepatocytes or with hUCBSCs (both 60%) (Figure 4(a)). The levels of human
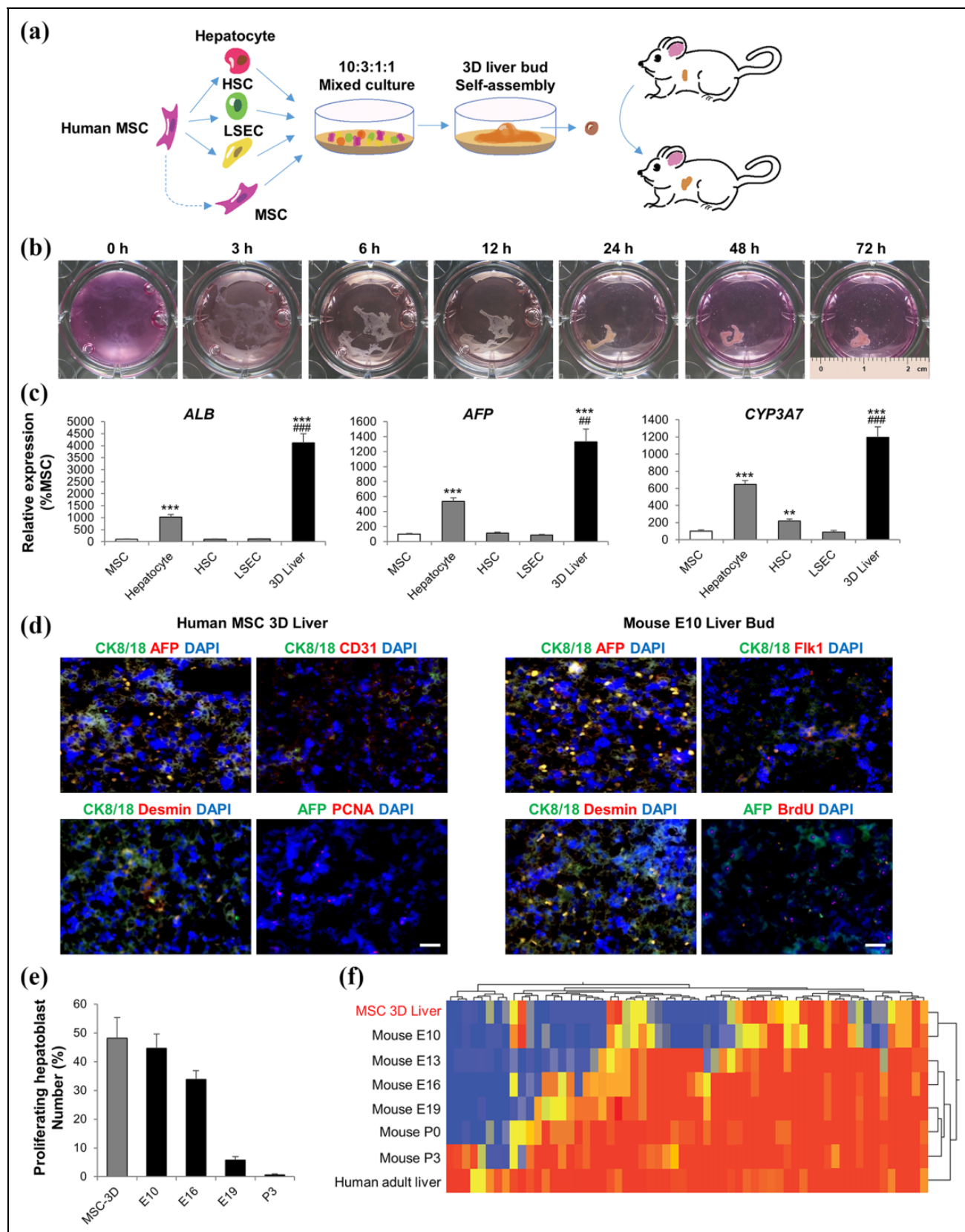
Figure 3. Human 3D liver bud assembly and function test from human umbilical cord blood stem cells (hUCBSCs). (a) Schematic representation of our strategy to assemble human 3D liver buds from naïve MSC and MSC-derived hepatocytes, HSC-like cells, and LSEC-like cells. (b) The time-lapse representative images of the self-assembly process. (c) Quantitative real-time PCR analysis of hepatic

albumin and AAT were also significantly higher during the entire experimental observation in the human liver bud-transplanted group compared to those of human adult hepatocyte- or hUCBSCs-transplanted groups (Figure 4(b,c)). To examine the expression of key functional proteins in transplanted liver buds and in alleviated mouse livers 30 days post-treatment, immunofluorescence for human ALB and CK8/18 were performed. In mouse livers transplanted with human MSCs or hepatocytes, the expression of ALB and CK8/18 were scarce, while in human liver buds their expressions were quite obvious (Figure 4(d)). In addition, we also tested the drug-metabolizing abilities of mice with or without hepatocyte/MSC/liver bud transplantation by challenging mice with ketoprofen or debrisoquine, which are known to be metabolized differently by mice and humans[18,19]. Results showed that when compared with sham, hepatocyte-, and MSC-transplanted mice, mice with liver bud transplantation exhibited the strongest metabolizing capabilities of both drugs (Figure 4(e,f)). To further characterize the maturation of transplanted human liver buds in comparison with newly generated human liver buds or adult human livers, the expression profiles of 38 mature liver signature genes were analyzed. The results showed that the expression profile of 30-day transplanted human livers was more similar to the one of adult human livers than the one of newly assembled human liver buds (Figure 5(a)). We then performed a quantitative real-time PCR analysis to validate the expression of nine key markers of mature livers in naïve hUCBSCs, newly generated human liver buds, 30-day transplanted human liver buds, adult human livers, and HepG2 hepatoma liver cells. The expression of those genes in transplanted human liver buds was similar to that in adult human livers (except AFP), and much higher than that in newly generated liver buds (Figure 5(b)). In conclusion, transplantation with self-assembled human liver buds could efficiently alleviate liver injury as they undergo *in vivo* maturation.

Discussion

In this report, we adopted a novel self-assembly strategy to generate functional 3D human liver buds from a mixture of differentiated hepatocyte-, HSC-, LSEC-like cells, and naïve human MSCs in an optimized 10:3:1:1 ratio. The 2D cultures of these mixed cell populations spontaneously form stable spheroidal 3D structures, possibly via a mesenchymal cell-driven condensation mechanism[23], since we and others have

proved that culturing stem cell-derived hepatocytes with HSCs or endothelial cells alone failed to form 3D transplantable tissues[18]. Newly generated human liver buds expressed markers of early-stage liver development, but they became similar to adult human livers 30 days after being transplanted into mice with acute liver failure. In addition, the mesenteric transplantation of human liver buds drastically alleviated hepatic injuries and rescued animals from liver failure-induced death.

"Organoid therapy" has recently been introduced as a novel approach for the treatment of clinically intractable diseases, such as end-stage liver diseases[24]. The first vascularized and functional human liver was generated in 2013 from an iPSC-derived organ bud transplant, which was obtained from a mixture of stem cells, hepatocytes, and human umbilical vein endothelial cells (HUVECs)[18]. Although not specifically tested, this protocol did not utilize HSCs, which are critical for the basic regulation of liver homeostasis[25]. Moreover, although vascularized, the physiological difference between LSECs and HUVECs for *in vitro* liver bud formation has not been evaluated[26]. To overcome these potential problems, we introduced for the first time a novel and efficient co-differentiation strategy that "transformed" nearly half of MSCs into HSC- and LSEC-like cells concurrently within 28 days by the sequential addition of growth factors and signal proteins into the culture medium. Functional tests confirmed the presence of HSC and LSEC basic characteristics (Figure 2). Importantly, we demonstrated that a physiologically relevant 10:3:3:1 ratio (hepatocytes: HSC-like cells: LSEC-like cells: naïve MSCs) produced functional and transplantable 3D liver buds within 72 h[27]. Our pilot study and other reports have proved that addition of LSECs and naïve MSCs to the cell mixture was indispensable for microvasculature formation and 3D structure condensation, respectively[18,23].

Unlike the conventional acute liver failure model, the ganciclovir-induced liver failure TK-NOG mouse model is more liver-specific and more compatible with the transplantation of exogenous human cells[22,28]. Treating mice with common toxins (e.g., thioacetamide) is also toxic to transplanted human cells. Mesenteric transplantation of 10 self-assembled human liver buds successfully rescued mice from death, which presents better injury amelioration and better hepatic protein production compared to splenic transplantation with naïve human MSCs or hepatocytes (Figure 4). Compared with orthotopic transplantation methods, the mesenteric transplantation model is less invasive and more clinically relevant because it does not affect the blood flow

Figure 3. (Continued). marker gene expression in human liver buds at day 3 of culture. (d) Representative images of immunostaining of CK8/18, AFP, CD31, Flk1, desmin, PCNA, and BrdU from 3D liver bud and mouse embryonic day 10 (E10) liver bud. Scale bars, 100 μm. (c) Percentage of proliferating hepatic cells calculated by dividing the number of PCNA/BrdU-positive cells by the number of CK8/18-positive cells. (d) Comparison of liver developmental gene signature genes among human liver bud, human adult liver tissue and mouse liver tissue of various developmental stages (from E10 to 3 weeks after birth). Data are presented as mean $\pm$ SEM, and significance was calculated by the Kruskal–Wallis test followed by Dunn's post hoc test (***P < 0.001 vs. MSC; #\#,###*P* < 0.01 or 0.001 vs. hepatocytes).
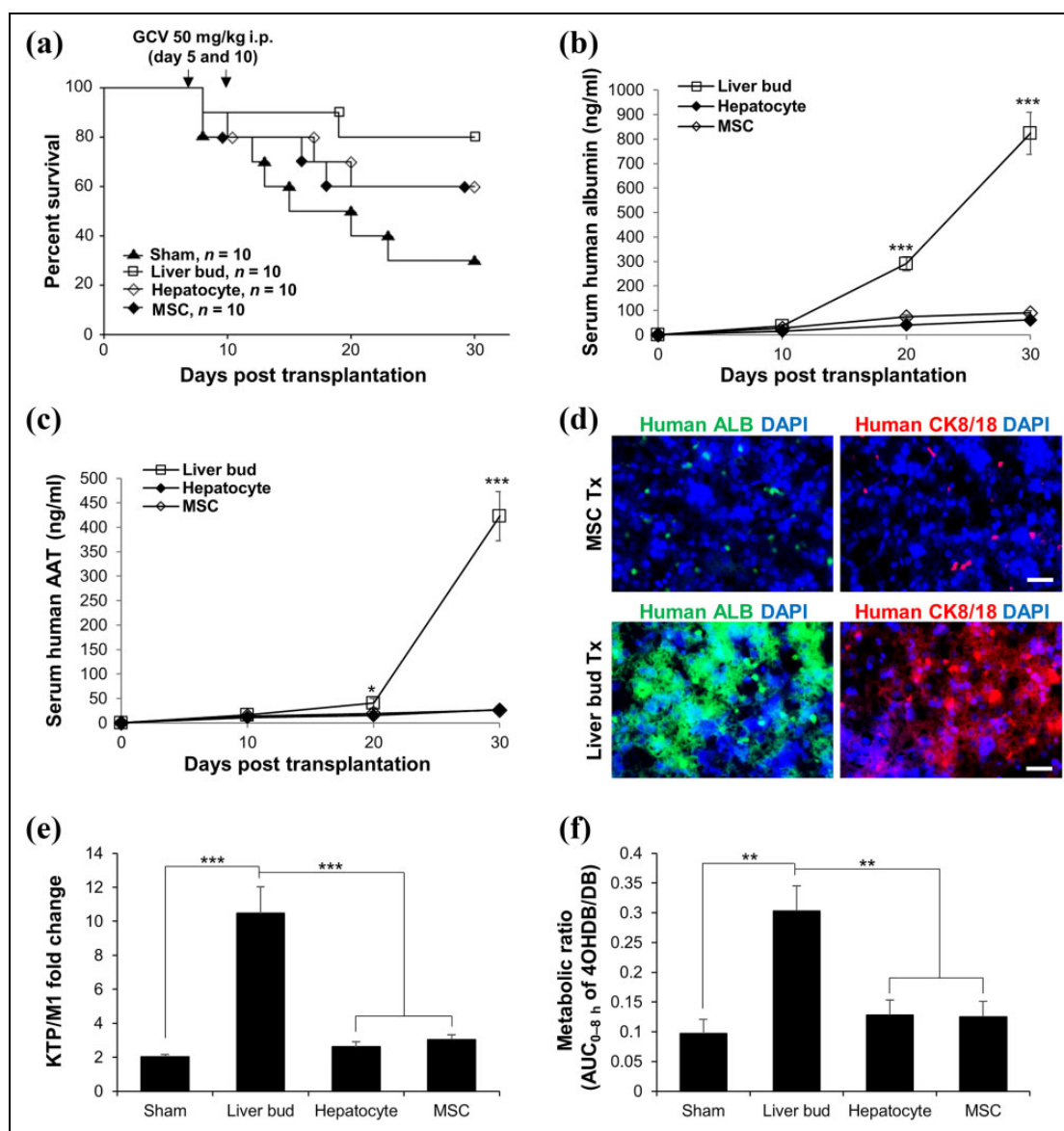
Figure 4. Mesenteric transplantation with assembled human 3D liver bud rescued acute liver failure in mice. (a) Kaplan–Meier survival curves of TK-NOG mice after liver injury induction, with or without human liver bud mesenteric transplantation, or hepatocytes/naïve MSC splenic transplantations for a 30-day observation. (b,c) Expressional changes of human albumin and alpha 1 antitrypsin (AAT) from TK-NOG mice after liver injury induction, with or without human liver bud mesenteric transplantation, or hepatocytes/naïve MSC splenic transplantations for a 30-day observation. (d) Representative immunofluorescence staining of liver bud (for mesenteric human liver bud transplantation) or host liver tissues (for hepatocytes/naïve MSC splenic transplantations) at day 30. Scale bars, 100 μm. (e,f) Changes of human-specific ketoprofen and debrisoquine metabolite formations in sham, liver bud-, hepatocyte-, and MSC-transplanted mice. For debrisoquine, metabolic ratios were calculated by dividing the $AUC_{0-8 \text{ h}}$ (the area under the curve from time 0 until 8 h) ratio of 4-hyroxydebrisoqune (4OHDB) to debrisoquine (DB). Data are presented as mean $\pm$ SEM, and significance was calculated by the Kruskal–Wallis test followed by Dunn's post hoc test (*,***$P < 0.05$ or 0.001 vs. day 0).

from the portal vein, which is considered to be important to improve hepatic functions[18,29]. After the ablation of transgenic host liver parenchymal cells at the appropriate time by ganciclovir administration, mesenteric transplants engrafted and matured most likely through the formation of a functional human vascular network. Indeed, due to the limited size of *in vitro* self-assembled liver buds ($\sim$4 mm in diameter), their size seemed to not be big enough to reverse the occurrence of hepatic failure beyond injury amelioration. Building a vascularized "bigger" liver tissue is necessary for future clinical applications.

In conclusion, we established a novel *in vitro* 3D self-assembly protocol to generate human liver buds derived from human MSCs, which is fast, reproducible, easy to
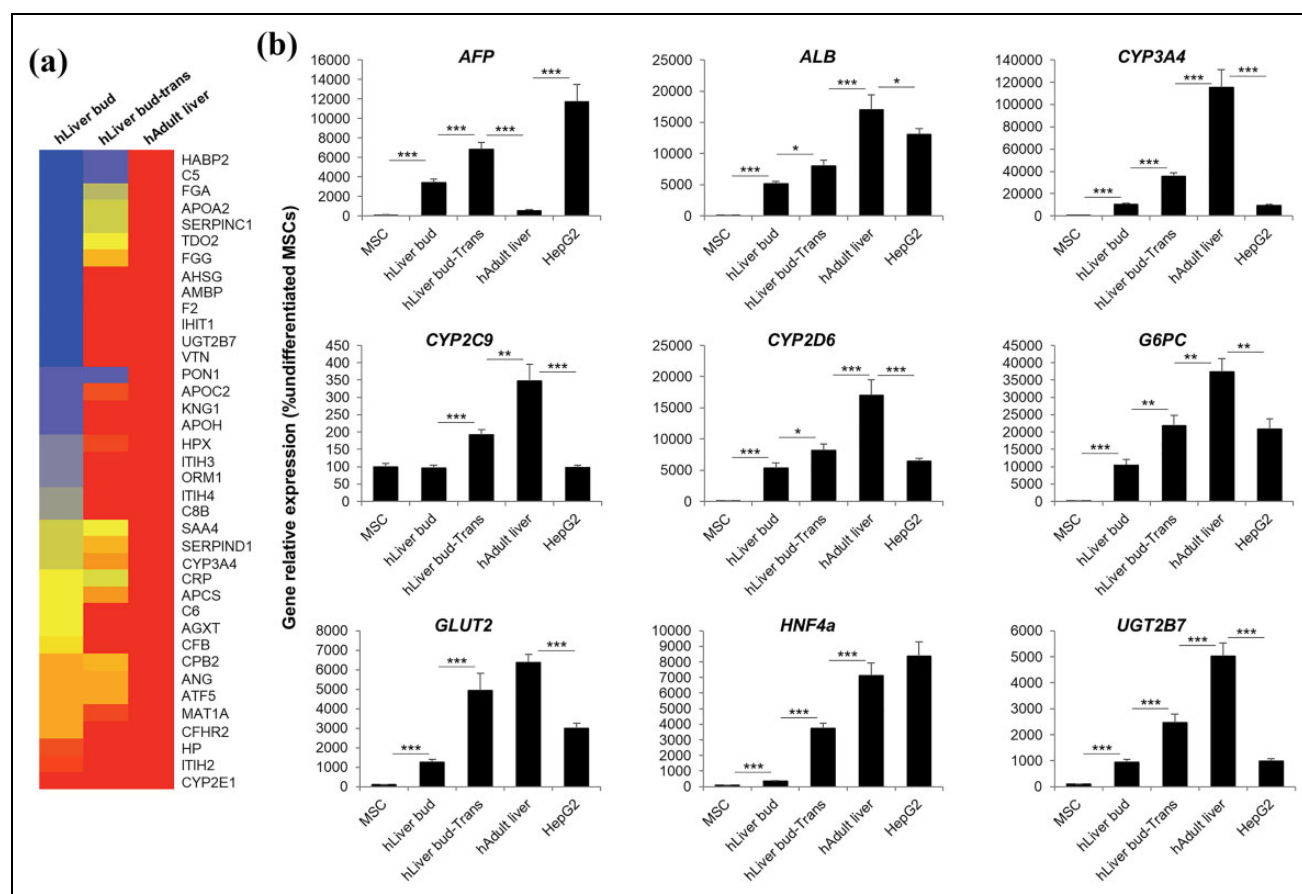
Figure 5. Signature gene expression profiles of mesenteric transplants of human liver bud. (a) Microarray analysis of mature liver marker genes in newly generated liver bud, transplanted (day 30) liver bud, and adult human liver tissue. (b) Quantitative real-time PCR analysis of key hepatic maturation genes showed that the mesenteric transplantation of human liver promoted its maturation. Data are presented as mean $\pm$ SEM, and significance was calculated by the Kruskal–Wallis test followed by Dunn's post hoc test (*,**,***P < 0.05, 0.01, or 0.001 between indicated groups).

follow, and which does not require a precoating step before differentiation. The generated human liver buds could undergo maturation and trigger therapeutic amelioration after their mesenteric transplantation into an acute liver failure mouse model. Importantly, we found that this protocol could be used also with human adipose-derived MSCs to generate 3D human liver buds (data not shown), which may significantly widen its application. Our method may facilitate future MSC-based multicellular "organoid" formation for therapeutic applications such as drug testing and regenerative medicine.

Author Contribution

Jing Li and Feiyue Xing contributed equally to this work.

Ethical Approval

This study was approved by and in accordance with the guidelines and regulations from the ethical committee of Shenzhen Third People's Hospital (No. 2016-07).

Statement of Human and Animal Rights

This article does not contain any studies with human subjects.

Statement of Informed Consent

There are no human subjects in this article and informed consent is not applicable.

Declaration of Conflicting Interests

The authors declared no potential conflicts of interest with respect to the research, authorship, and/or publication of this article.

Supplemental Material

Supplementary material for this article is available online.

References

1. Xu J, Murphy SL, Kochanek KD, Bastian BA. Deaths: Final Data for 2013. Natl Vital Stat Rep. vol 65 no 2. Hyattsville, MD: National Center for Health Statistics. 2016. http://www.cdc.gov/nchs/data/nvsr/nvsr64/nvsr64_02.pdf (2016, accessed 1 December 2017).

2. Fisher RA. Living donor liver transplantation: Eliminating the wait for death in end-stage liver disease? Nat Rev Gastroenterol Hepatol. 2017;14(6):373–382.

3. Mazza G, De Coppi P, Gissen P, Pinzani M. Hepatic regenerative medicine. J Hepatol. 2015;63(2):523–524.

4. Nagamoto Y, Takayama K, Ohashi K, Okamoto R, Sakurai F, Tachibana M, Kawabata K, Mizuguchi H. Transplantation of a human iPSC-derived hepatocyte sheet increases survival in mice with acute liver failure. J Hepatol. 2016;64(5):1068–1075.

5. Shulman M, Nahmias Y. Long-term culture and coculture of primary rat and human hepatocytes. Methods Mol Biol. 2013;945:287–302.

6. Zhou R, Li Z, He C, Li R, Xia H, Li C, Xiao J, Chen ZY. Human umbilical cord mesenchymal stem cells and derived hepatocyte-like cells exhibit similar therapeutic effects on an acute liver failure mouse model. PLoS One. 2014;9(8):e104392.

7. Shi M, Zhang Z, Xu R, Lin H, Fu J, Zou Z, Zhang A, Shi J, Chen L, Lv S, He W, et al. Human mesenchymal stem cell transfusion is safe and improves liver function in acute-on-chronic liver failure patients. Stem Cells Transl Med. 2012;1(10):725–731.

8. El-Ansary M, Abdel-Aziz I, Mogawer S, Abdel-Hamid S, Hammam O, Teaema S, Wahdan M. Phase II trial: Undifferentiated versus differentiated autologous mesenchymal stem cells transplantation in Egyptian patients with HCV induced liver cirrhosis. Stem Cell Rev. 2012;8(3):972–981.

9. Spahr L, Lambert JF, Rubbia-Brandt L, Chalandon Y, Frossard JL, Giostra E, Hadengue A. Granulocyte-colony stimulating factor induces proliferation of hepatic progenitors in alcoholic steatohepatitis: A randomized trial. Hepatology. 2008;48(1):221–229.

10. Gasbarrini A, Rapaccini GL, Rutella S, Zocco MA, Tittoto P, Leone G, Pola P, Gasbarrini G, Di Campli C. Rescue therapy by portal infusion of autologous stem cells in a case of drug-induced hepatitis. Dig Liver Dis. 2007;39(9):878–882.

11. Wang L, Li J, Liu H, Li Y, Fu J, Sun Y, Xu R, Lin H, Wang S, Lv S, Chen L, et al. Pilot study of umbilical cord-derived mesenchymal stem cell transfusion in patients with primary biliary cirrhosis. J Gastroenterol Hepatol. 2013;28(suppl 1):85–92.

12. Sang W, Lv B, Li K, Lu Y. Therapeutic efficacy and safety of umbilical cord mesenchymal stem cell transplantation for liver cirrhosis in Chinese population: a meta-analysis. Clin Res Hepatol Gastroenterol. 2018;42(3):193–204.

13. Abdel Aziz MT, El Asmar MF, Atta HM, Mahfouz S, Fouad HH, Roshdy NK, Rashed LA, Sabry D, Hassouna AA, Taha FM. Efficacy of mesenchymal stem cells in suppression of hepatocarcinorigenesis in rats: Possible role of Wnt signaling. J Exp Clin Cancer Res. 2011;30:49.

14. Huppert SS, Campbell KM. Emerging advancements in liver regeneration and organogenesis as tools for liver replacement. Curr Opin Organ Transplant. 2016;21(6):581–587.

15. Blaner WS, O'Byrne SM, Wongsiriroj N, Kluwe J, D'Ambrosio DM, Jiang H, Schwabe RF, Hillman EM, Piantedosi R, Libien J. Hepatic stellate cell lipid droplets: A specialized lipid droplet for retinoid storage. Biochim Biophys Acta. 2009;1791(6):467–473.

16. Geerts A, Niki T, Hellemans K, De Craemer D, Van Den Berg K, Lazou JM, Stange G, Van De Winkel M, De Bleser P. Purification of rat hepatic stellate cells by side scatter-activated cell sorting. Hepatology. 1998;27(2):590–598.

17. Huggett JF, Foy CA, Benes V, Emslie K, Garson JA, Haynes R, Hellemans J, Kubista M, Mueller RD, Nolan T, Pfaffl MW, et al. The digital MIQE guidelines: Minimum information for publication of quantitative digital PCR experiments. Clin Chem. 2013;59(6):892–902.

18. Takebe T, Sekine K, Enomura M, Koike H, Kimura M, Ogaeri T, Zhang RR, Ueno Y, Zheng YW, Koike N, et al. Vascularized and functional human liver from an iPSC-derived organ bud transplant. Nature. 2013;499(7459):481–484.

19. Yu AM, Idle JR, Gonzalez FJ. Polymorphic cytochrome P450 2D6: Humanized mouse model and endogenous substrates. Drug Metab Rev. 2004;36(2):243–277.

20. Matsumoto K, Yoshitomi H, Rossant J, Zaret KS. Liver organogenesis promoted by endothelial cells prior to vascular function. Science. 2001;294(5542):559–563.

21. Gouysse G, Couvelard A, Frachon S, Bouvier R, Nejjari M, Dauge MC, Feldmann G, Henin D, Scoazec JY. Relationship between vascular development and vascular differentiation during liver organogenesis in humans. J Hepatol. 2002;37(6):730–740.

22. Hasegawa M, Kawai K, Mitsui T, Taniguchi K, Monnai M, Wakui M, Ito M, Suematsu M, Peltz G, Nakamura M, Suemizu H. The reconstituted "humanized liver" in TK-NOG mice is mature and functional. Biochem Biophys Res Commun. 2011;405(3):405–410.

23. Takebe T, Enomura M, Yoshizawa E, Kimura M, Koike H, Ueno Y, Matsuzaki T, Yamazaki T, Toyohara T, Osafune K, Nakauchi H, et al. Vascularized and complex organ buds from diverse tissues via mesenchymal cell-driven condensation. Cell Stem Cell. 2015;16(5):556–565.

24. Lancaster MA, Knoblich JA. Organogenesis in a dish: Modeling development and disease using organoid technologies. Science. 2014;345(6194):1247125.

25. Yin C, Evason KJ, Asahina K, Stainier DY. Hepatic stellate cells in liver development, regeneration, and cancer. J Clin Invest. 2013;123(5):1902–1910.

26. Poisson J, Lemoinne S, Boulanger C, Durand F, Moreau R, Valla D, Rautou PE. Liver sinusoidal endothelial cells: Physiology and role in liver diseases. J Hepatol. 2017;66(1):212–227.

27. Juza RM, Pauli EM. Clinical and surgical anatomy of the liver: A review for clinicians. Clin Anat. 2014;27(5):764–769.

28. Kosaka K, Hiraga N, Imamura M, Yoshimi S, Murakami E, Nakahara T, Honda Y, Ono A, Kawaoka T, Tsuge M, Abe H, et al. A novel TK-NOG based humanized mouse model for the study of HBV and HCV infections. Biochem Biophys Res Commun. 2013;441(1):230–235.

29. Chen AA, Thomas DK, Ong LL, Schwartz RE, Golub TR, Bhatia SN. Humanized mice with ectopic artificial liver tissues. Proc Natl Acad Sci U S A. 2011;108(29): 11842–11847.